ISSN 1075-7015, Geology of Ore Deposits, 2024, Vol. 66, No. 8, pp. 1133–1144. © Pleiades Publishing, Ltd., 2024.
Russian Text © The Author(s), 2023, published in Zapiski Rossiiskogo Mineralogicheskogo Obshchestva, 2023, No. 4, pp. 47–64.

MINERALS AND MINERAL PARAGENESES

Neotocite from Manganese Ores of the Ushkatyn-III Deposit, Central Kazakhstan

A. I. Brusnitsyn[a], * and G. S. Egorov[a]

[a] *Department of Mineralogy, St. Petersburg State University, Saint Petersburg, 199115 Russia*

**e-mail: a.brusnitsin@spbu.ru*

Received May 10, 2023; revised May 17, 2023; accepted June 14, 2023

Abstract—Neotocite, an X-ray amorphous hydrous manganese silicate, is the mineral typical of low-grade metamorphosed sedimentary manganese ores of the Ushkatyn-III deposit in Central Kazakhstan. It occurs both in the ore groundmass, where it associates with hausmannite, tephroite, caryopilite, friedelite, pennantite, rhodochrosite, kutnohorite, and some other minerals, as well as in veinlets crossing these ores. In the veinlets, segregations of homogeneous neotocite reach several cubic centimeters in size. The study of such large segregations allows us to characterize optical, mechanical and thermal properties, IR spectra, and chemical composition of neotocite using modern analytical methods. It is assumed that manganese in the neotocite is mainly (or even completely) divalent. The stoichiometry of the mineral with allowance for the chemical and thermal analyses and IR spectroscopic data corresponds to the ideal formula $Mn_7(Si_8O_{20})(OH)_6 \cdot nH_2O$. This formula reliably reflects the silicon to manganese ratio in the mineral, its layered crystal structure, and at least two different hydrogen speciations: (OH)-groups and H_2O molecules. The above-given formula of neotocite could be accepted as the idealized one. Neotocite was formed at low temperature reducing conditions during the burial of metal-bearing deposits containing a Mn–Si–H_2O substance (gel?), or later through the hydrothermal alteration of already formed manganese ores.

Keywords: neotocite, minerals of manganese ores, sedimentary manganese deposits, Ushkatyn-III deposit

DOI: 10.1134/S1075701524700247

INTRODUCTION

Neotocite is an X-ray amorphous hydrous manganese silicate. At present, this mineral is accepted as mineral species, but frequently is considered as hydrated Mn–Si glass or as Mn–Si–H_2O mineraloid. Neotocite was noted for the first time by N. Nordenskiöld at the Erik-Ers Mine in Sweden (Nordenskiöld, 1849). Later, the glass-like Mn–Si substance was also called *penwithite, stratopeite, wittingite, sturtite*, and some others. However, the comparison of physical characteristics and chemical compositon of all varieties of "Mn–Si glass" revealed their great similarity. Based on this fact, the initial term *neotocite* was accepted, while all other names were canceled (Clark et al., 1978; *Mineraly,* 1992; Strunz and Nickel, 2001).

The transmission electron microscopic study of neotocite revealed the presence of disoriented fragments of layer structure (Eggleton et al., 1983). Based on these data, the neotocite is characterized by a loose packing of 50–100 Å spheres with a shell formed by alternating layers of SiO_4-tetrahedra and MnO_6-octahedra, while the inner space is likely filled with hydrated amorphous substance or is empty. The spheres are connected into a physically isotropic substance with a porosity about 10 vol %. The presence of fragments of layer structure in the neotocite is also confirmed by IR spectroscopy (Wheland and Goldich, 1961; Clark et al., 1978; *Mineraly,* 1992; Povondra, 1996; Brusnitsyn, 2000; Chukanov, 2014). Therefore, neotocite is sometimes ascribed to layer silicates of 1 : 1 structural type (kaolinite type) (Strunz and Nickel, 2001).

Neotocite in general is not a scarce mineral. It occurs in rocks of different composition and genesis as subordinate or accessory component, but the majority of its finds are confined to the manganese-bearing deposits, where it is formed either as a product of diagenetic coagulation of Mn–Si–H_2O gel, or as late hydrothermal phase, or (rarely and frequently ambiguously) as supergene mineral in the oxidation zone (Akelsiev, 1960; Clark et al., 1978; Andrushchenko et al., 1985; Roi, 1986; *Mineraly,* 1992; Povondra, 1996; Brusnitsyn, 2000, 2013; Brusnitsyn and Chukanov, 2001; Brusnitsyn et al., 2018). In all cases, the amorphous state of neotocite and the appearance of only fragments of layer crystalline structure are explained by disproportion between large MnO_6-octahedra and small SiO_4-tetrahedra, which cannot be compensated at rapid low-temperature mineral formation and high ovsersaturation of the parent solution.

Neotocite is frequently mentioned in manganese rocks, but publications dedicated to this mineral are few in number. This is mainly related to the fact that neotocite is usually represented by glassy aggregates unevenly distributed among groundmass minerals or composing thin veinlets. These aggregates are difficult to study, while obtained information is usually fragmentary and not always correct. Therefore, the scarce finds of large neotocite aggregates deserve special attention. Such neotocite accumulations were found by us in the manganese ores of the Ushkatyn-III deposit in Central Kazakhstan. Neotocite (called penwitite) has been already mentioned in this deposit by first researchers as one of the widespread minerals, locally as "the main ore component" (Kayupova, 1974). Results of our works in general confirm these data. Moreover, in 2018, we found samples with veins consisting of homogenous neotocite up to a few cm long and 1 cm thick. This material offered opportunity to specify the physical properties and chemical composition of neotocite using modern analytical methods. In addition, the study of neotocite-bearing mineral assemblages made it possible to estimate some conditions of formation of manganese ores.

BRIEF CHARACTERISTICS OF THE DEPOSIT

The Ushkatyn-III deposit is situated 300 km southwest of Karaganda, 15 km northeast of the Zhairem settlement. It was discovered in 1962 and has been explored since 1982. The deposit is complex in composition: carbonate units in its different parts contain hydrothermal barite–lead ores and low-grade metamorphosed hydrothermal-sedimentary manganese and iron ores (Kayupova, 1974; Buzmakov et al., 1975; Rozhnov, 1982; Kalinin, 1985; Brusnitsyn et al., 2021b).

The deposit is confined to the paleorift structure filled with the Upper Devonian–Lower Carboniferous terrigenous–siliceous–carbonate sedimentary rocks. From the northeast to the southwest of the deposit, the red-colored sandstones and siltstones subsequently give way to the reef organogenic–algal limestones and products of their destruction (calcareous siltstones, sandstones, and sedimentogenic breccias) and further to the laminated organogenic–detrital limestones. The reef limestones host superimposed pocket–reticulate and vein-disseminated barite–lead (barite–galena) mineralization. The organogenic–detrital limestones contain series of beds (different sections of the unit include from 5 to 14 beds) of iron and manganese ores that are syngenetic to host carbonate rocks.

The iron and manganese ores represent fine-grained lenticular-banded and laminated rocks. The iron ores are mainly formed by hematite, calcite, and quartz with small amounts of albite, muscovite, barite, apatite, tilasite, pyrite, and galena. Based on major minerals, the manganese ores are subdivided into two types (the names are given after minerals that are of interest as manganese source): hausmannite and braunite types (Kayupova, 1974; Brusnitsyn et al., 2021a). The major minerals of hausmannite ores are hausmannite, rhodochrosite, calcite, tephroite, manganese members of the humite group (sonolite and alleganite), and friedelite, while subordinate minerals are hematite, jacobsite, caryopilite, clinochlore, and pennantite. The braunite ores are mainly made up of braunite and calcite, locally with quartz and albite, while typical subordinate minerals are hematite, kutnohorite, rhodochrosite, parsettensite, kayupovaite, friedelite, pennatite, rhodonite, manganaxinite, and K-feldspar.

The mineral composition of the ores was formed during low-grade metamorphism ($T = 250 \pm 50$°C, $P = 2 \pm 1$ kbar) of metalliferous sediments made up of iron and manganese oxides, carbonate material of "background" sediments, with admixture of siliceous, aluminosilicate, and organic matters. Differences in the mineral composition of manganese ores are determined by inequal content of reactive organic matter (OM) in starting sediments. The braunite ores are formed under oxidizing conditions after practically OM-free sediments, while hausmannite ores (with tephroite and rhodochrosite) were produced under reducing subanaerobic conditions provided by microbial destruction of OM buried in sediments (Brusnitsyn et al., 2020, 2021a).

MATERIALS AND METHODS

Materials for studies. Samples for this work were collected by us in 2018 in the southwestern part of the Ushkatyn-III quarry, where the unit of the iron- and manganese-bearing sediments is best recovered. In total, we studied over 100 ore samples, including 10 samples containing neotocite. All samples were studied by optical and electron microscopy. Detailed studies using all methods were made for neotocite from large vein cutting across the hausmannite ore (sample Ush318-113).

Mineralogical study of samples. A complex of traditional methods used for this study included optical microscopy in transmitted and reflected light, X-ray phase analysis, electron microscopy coupled with energy-dispersive X-ray analysis, thermal (DSC and TG) analysis, and IR-spectroscopy.

The initial identification of minerals was carried out at the Department of Mineralogy in St. Petersburg State University using a Leica DM2500P optical microscope. The study of polished sections was carried out in two resource centers (RC) of St. Petersburg State University: "Microscopy and Microanalysis" and "Geomodel". In the RC "Microscopy and Microanalysis", minerals were identified and photographed in the polished sections using a scanning electron microscope (SEM) HITACHI TM 3000

equipped with EDS OXFORD. The chemicall analysis of minerals was carried out in the RC "Geomodel" using a SEM Hitachi S-3400N microscope equipped with EDS Oxford Instruments AzTec Energy X-Max 20. The EDS spectra were obtained at an accelerating voltage of 20 kV, a beam current of 2 nA, and counting time of 60 s. Natural and synthetic compounds were used as standards. The analyses were carried out by A.I. Brusnitsyn, G.S. Egorov, N.S. Vlasenko, and V.V. Shilovskhikh.

X-ray phase analyses, thermal X-ray diffraction, thermal analysis, and IR spectroscopy were conducted at the RC "X-ray Diffraction Methods of Study" of the St. Petersburg State University. The powder diffraction patterns were obtained on an Rigaku Mini Flex II diffractometer with CuK_α-radiation. The samples were recorded within an angle intervals 2θ from 5° to 60° at a rate of 2θ/min, analyst G.S. Egorov. Thermal X-ray diffraction was made in a high-temperature Rigaku "SHT-1500" camera with a resistive heater, at air temperature up to 900°C, a a heating step of 100°C up to 500°C and 20°C at higher temperatures. Phases were recorded using built-in diffractometer with Co-anode, analyst M.G. Krzhizhanovskaya.

The behavior of sample at heating (differential scanning calorimetry and thermogravimetric analysis) was studied using a Netzsch STA 449 F3 derivatograph in a platinum crucible. The samples were recorded within a range of 30–1200°C in atmosphere at heating rate of 10°C/min, analysts G.S. Egorov and O.G. Bubnova.

IR spectroscopic study was carried out on a Bruker Vertex 70 spectrophotometer. Approximately 2 mg of neotocite was mixed with 200 mg of powdered KBr and pressed in pellets. The transmission spectra were recorded at 64 scan/s and a resolution of 2 cm^{-1}. Data were processed using an Opus software. Analysts G.S. Egorov and O.G. Bubnova.

RESULTS AND DISCUSSION

Assemblages and morphology of neotocite. At the Ushkatyn-III deposit, neotocite occurs only in hausmannite ores and was not established in association with braunite. In the typical (prevailing) varieties of the hausmannite ores, neotocite is relatively scarce mineral usually amounting no more than 1–3 vol %. In the groundmass of such ores, neotocite forms irregular in shape equant grains filling interstices between grains of rhodochrosite, calcite, hausmannite, pennantite, tephroite, and some other minerals (Figs. 1a, 1b). Judging from structures of mineral aggregates, the neotocite is formed one of the last minerals, either cementing existing pores or partly replacing earlier silicate, being confined mainly to the grain boundaries. The neotocite occurs not only in the groundmass, but also in late veinlets, which are up to 0.3 mm thick and 3 cm long. Locally, neotocite (both in the groundmass and in veinlets) is replaced by plates of friedelite and fancy capillary dendrites of rhodochrosite. The replacement of neotocite is best expressed in the late veinlets (Figs. 1c–1f).

In addition to the above-mentioned ores, the Ushkatyn-III deposit contains a relatively scarce variety of hausmannite ores, where neotocite reaches rock-forming amounts (up to 20 vol %). This variety represents cryptocrystalline dark brown rock with unevenly patchy, vaguely banded, sometimes, veined-reticulate structure (Fig. 2). The groundmass is made up of hausmannite, neotocite, caryopilite, tephroite, rhodochrosite, and kutnohorite, while subordinate and accessory minerals are hematite, jacobsite, rutile, cerianite-(Ce), pennantite, talc, calcite, barite, and sarkinite. Thus, the mineral composition of these ores in general corresponds to the typical hausmannite ores of the deposit, but with addition of neotocite. The neotocite-rich ores have a heterogeneous texture with complex and ambiguous spatiotemporal relations between minerals. Locally, the structure of mineral aggregates could be considered as result of replacement of the earlier neotocite by manganese serpentine, caryopilite (Figs. 3a, 3b). Such relations are possible in the adjacent areas, but are not obvious. Especially complex pattern is observed in sites where ores are made up of three and more minerals (Figs. 3c–3f). Neotocite could be both relict phase, which is replaced by caryopilite, and, in contrast, the latest phase replacing the early caryopilite. In this case, thin reticulate caryopilite in neotocite could be considered as relicts of initial felted-scaled manganese serpentine in a newly formed glassy phase. In addition, these ores are also intersected by late veinlets, which are almost completely made up of neotocite, while subordinate minerals are rhodochrosite, barite, and sarkinite. These ores contain veinlets of maximum sizes, samples from which were used to obtain main characteristics of the Ushkatyn neotocite.

Physical properties. In samples, neotocite is identified by typical glassy appearance. Mineral color varies from saturated reddish brown to light yellow. On air, the mineral becomes gradually darker and grades into black, which indicates manganese oxidation. In unoxidized samples, neotocite is transparent in thin chips, with greasy luster. The mineral is soft, brittle, with conchoidal fracture. In the transmitted light, the neotocite is light yellow, sometimes shows uneven cloudy distribution of tints. The mineral is most frequently optically isotropic, but locally shows a very weak birefringence, with refractive index varying from 1.425 in dark brown to 1.488 in light brown domains. Numerous syneresis cracks are practically always well discernible in polished thin sections.

Results of thermal analysis. Previous researchers noted two thermal effects in the DTA curve: endothermic peak at 150° and exothermic peak at 800° (Kayupova, 1974). Our studies refined these data.

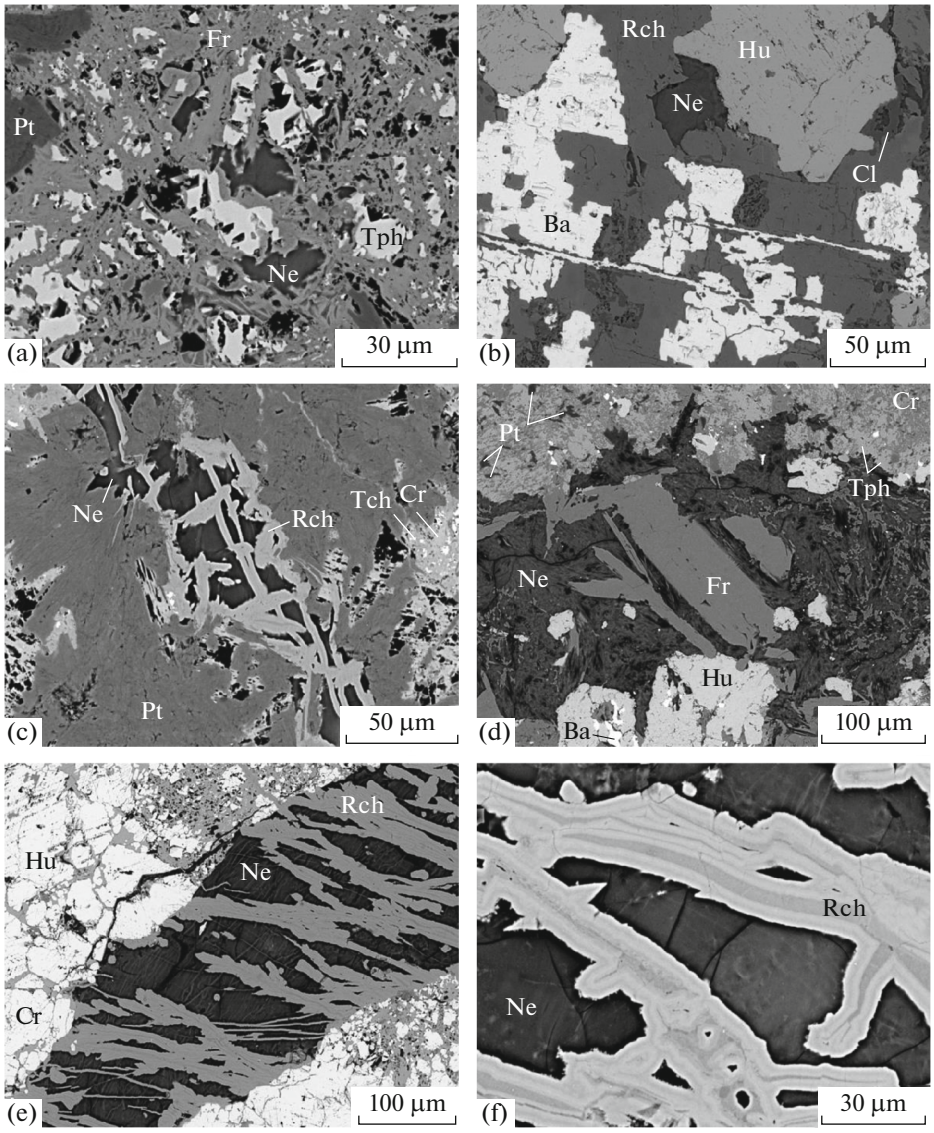

Fig. 1. Morphology of neotocite aggregates from typical varieties of hausmannite ores. Photos of polished sections in reflected electrons. Presented are varieties of hausmannite ores with low contents of neotocite: (a and b) groundmass minerals, morphologically irregular neotocite in the tephroite–friedelite (a) and hausmannite–rhodochrosite (b) aggregates; (c–f) minerals of late veinlets: (c) filiform segregations of rhodochrosite in the neotocite veinlets cutting pennantite aggregates; (d) lamellar crystals of friedelite in neotocite veinlet developed in the groundmass made up of pennatite, caryopilite, tephroite, and hausmannite; (e and f) dendritic capillary segregations of rhodochrosite in the neotocite veinlet cutting across the caryopilite–hausmannite mass; (e) a general view; (f) detail. Gradations of gray rhodochrosite color reflect the variations of manganese and calcium in the mineral (lighter zones are more enriched in manganese than darker zones). Minerals: (Hu) hausmannite, (Tph) tephroite, (Cr) caryopilite, (Fr) friedelite, (Pt) Pennantite, (Ne) Neotocite, (Cl) calcite, (Rch) rhodochrosite, (Ba) barite.

The DSC of the studied neotocite (Fig. 4) is characterized by the intense and wide endothermic peak with T_{max} = 130°C, which indicates the presence of weakly bound crystallization water molecules as well as two peaks caused by phase transformations of matter: exothermic peak at T_{max} = 791°C and endothermic peak at T_{max} = 1098°C. The first peak is related to the formation of braunite, while the second, is likely corresponds to rhodonite or similar silicate (*Mineraly,* 1992). The appearance of braunite is confirmed by the thermal X-ray diffraction. Diagnostic reflections typical of this mineral d(Å)/I: 3.49/15, 2.70/100, 2.35/20, 2.15/15, 1.66/30, and 1.42/15 are observed in the diffraction pattern of heated neotocite starting from temperature 740°C and are very clearly identified at temperatures 800°C and more. The TG curve of neotocite records a jump-like weight loss at T_{max} = 130°C (–4%) and T_{max} = 1098°C (–1%), in addition, a gradual weight loss (–5.5%) within an interval T = 200–600°C reflects the removal of molecular water (in the same

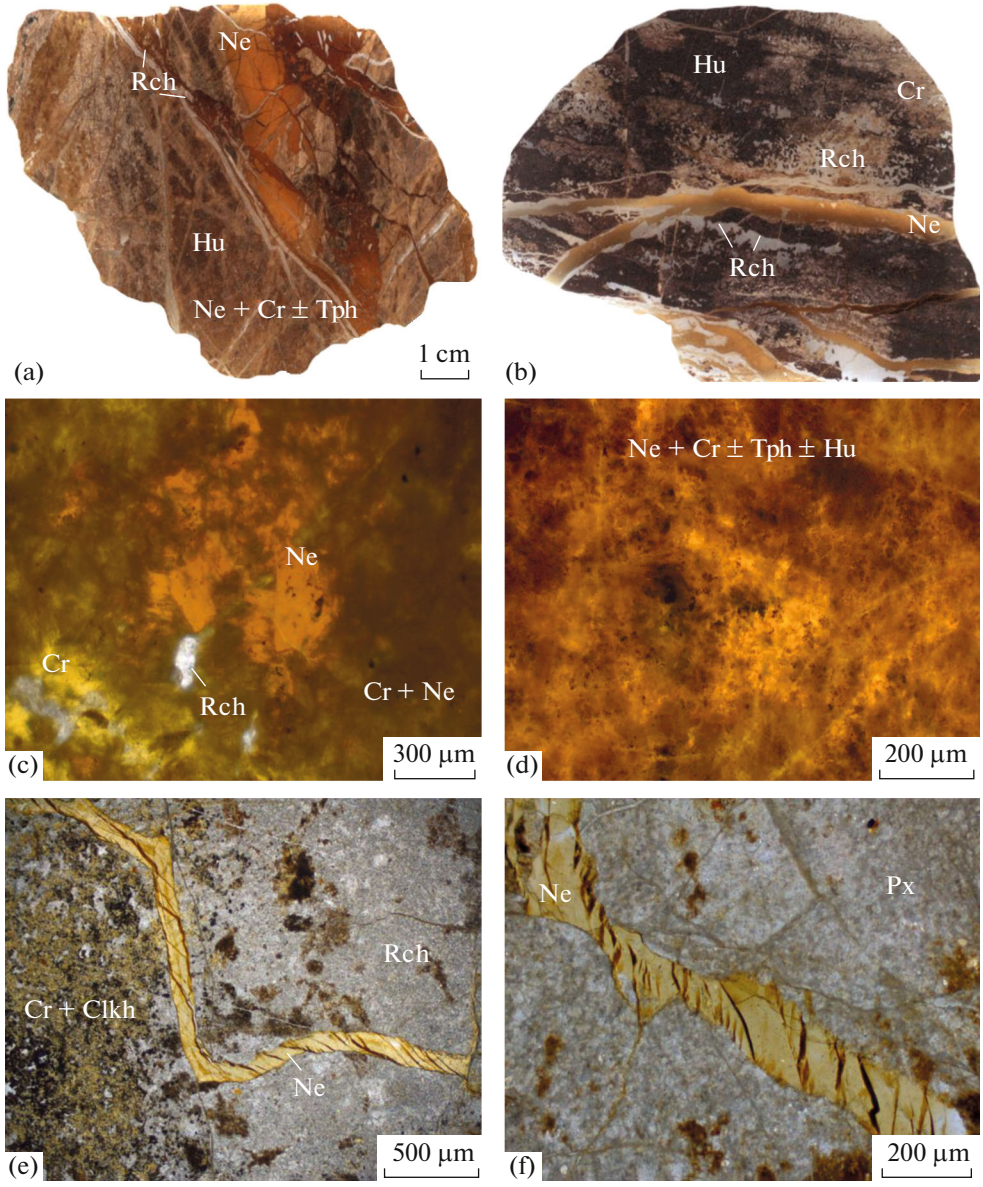

Fig. 2. Morphology of neotocite segregations in the hausmannite ores with high contents of this mineral. Photographs: (a and b) samples in a single scale; (c–f) polished thin sections without analyzer. (a–d) varieties of hausmannite ores with high content of neotocite. (a) groundmass of the rock is made up of neotocite and caryopilite with inclusions of tephroite and hausmannite, lenticular-vein segregations of homogenous neotocite are seen in the upper right part of the photo; (b) neotocite veinlets in hausmannite ore; (c and d) glassy cryptocrystalline groundmass of the rock made up mainly of neotocite and caryopilite; (e and f) neotocite veinlets in the rhodochrosite mass. Minerals: (Hu) hausmannite, (Tph) tephroite, (Cr) caryopilite, (Clkh) clinochlore, (Ne) neotocite, (Rch) rhodochrosite.

temperature interval, the DSC curve records a clear gentle slope). The total decrease of sample weight at its heating from 20 to 1020°C accounted for 11.90 wt %.

Infrared spectroscopy. The IR spectrum of neotocite contains several absorption bands of different intensity (Fig. 5). The position of main most intense absorption band at 1018 cm^{-1} (stretching vibrations of Si–O bonds) corresponds to a stoichiometry of anionic radical of layer silicates O : Si = 2.6 ± 0.1 (Chukanov, 1995, 2014). Bands at 3450 and 1637 cm^{-1} indicate the presence of weakly bound crystallization (or zeolitic) water, while band at 3636 $см^{-1}$ corresponds to OH-group. The absorption bands of water are wide and asymmetric, which may indicate the diversity of its sites and speciation in the neotocite. Similar IR spectra are also typical of neotocite from other deposits, as well as of series of layer silicates, in particular, caryopilite, parsenttensite, stilpnomelane, smectites (saponite, saukonite), shamosite, and some other minerals. Such similarity of IR spectra of neotocite

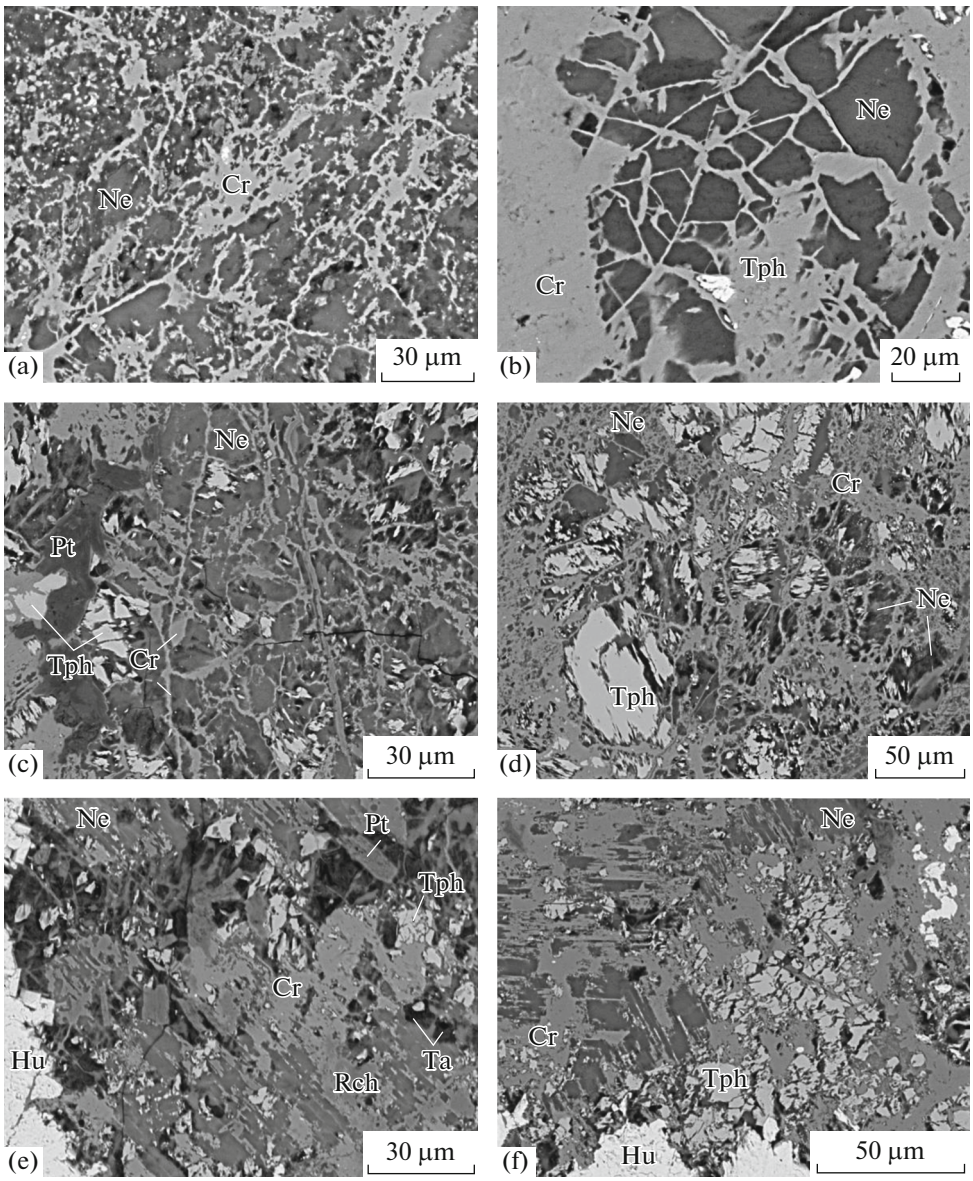

Fig. 3. Mutual relations between minerals in the neotocite-rich varieties of hausmannite ores. BSE photos of polished sections. Presented are ore varieties with high neotocite contents (see samples and polished thin sections in Figs. 2a–2d). (a and b) arachnoid (a) and reticulate (b) segregations of caryopilite (light) in neotocite (dark); (c–f) groundmass of the rock made up of neotocite, caryopilite, tephroite, hausmannite, pennantite, and talc. It is seen in photos (a–c) that reticulate caryopilite is developed after neotocite, but in photos d–f such relationships between these minerals are not obvious. Minerals: (Hu) hausmannite, (Tph) tephroite, (Cr) caryopilite, (Pt) Pennantite, (Ta) talc, (Ne) Neotocite, (Rch) rhodochrosite.

and layer silicates was also noted by previous researchers (Wheland and Goldich, 1961; Clark et al., 1978; *Mineraly,* 1992; Povondra, 1996; Brusnitsyn, 2000; Chukanov, 2014).

X-ray characteristics. X-ray diffraction pattern of the Ushkatyn neotocite contains five wide diffuse peaks with maxima at 4.3, 3.7, 2.76, 2.56, and 1.61 Å (Fig. 6). The X-ray patterns of neotocite from other deposits also show from three to six poorly expressed maxima with "low" or "very low" intensity, while interplanar spacings of three most intense peaks are 3.5, 2.6, and 1.6 Å (Wheland and Goldich, 1961; Clark et al., 1978; *Mineraly,* 1992). In combination with IR spectroscopic data, this indicates that the atomic structure of neotocite is not fully amorphous, but contains fragments of molecular packages. The diffraction patterns of such type are observed in the disordered minerals of the asbolane group and some other manganese hydroxides (Chukhrov et al., 1989).

Owing to the steep hump-like rise of background level within angle intervals $2\theta = 20°–28°$ and, espe-

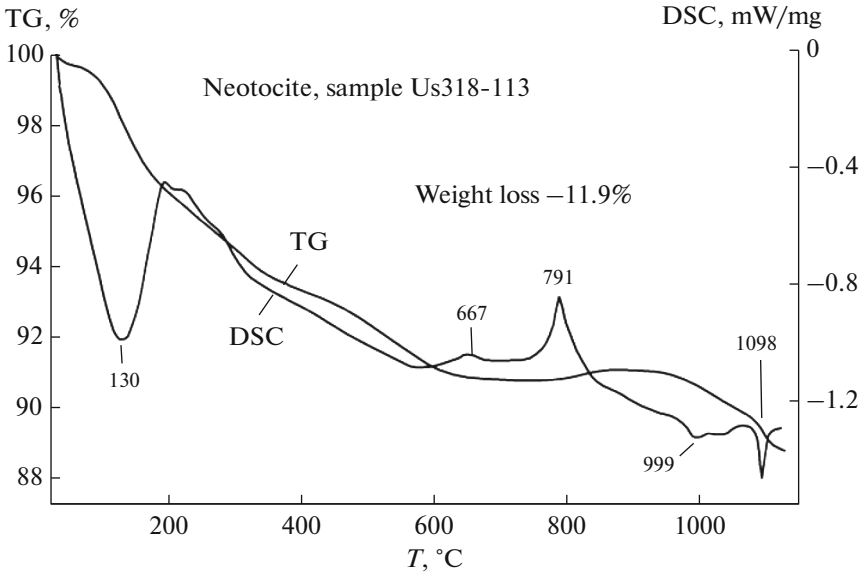

Fig. 4. Results of thermal analysis of neotocite: DSC and TG curves.

cially, 30°–38°, the neotocite can be identified even in polymineral samples

Chemical composition of the studied neotocite is sufficiently stable and characterized by the high silicon and manganese contents, and low contents of aluminum, magnesium, calcium, and sodium (Table 1). The total SiO_2 + MnO^{tot} accounts for approximately 85 wt %, while the total content of other components is less than 3 wt %. Trace elements are dominated by magnesium (up to 1.5 wt % MgO) and calcium (up to 1.1 wt % CaO). In all analyses, the iron concentration was below the detection limit of energy dispersive detector. Significant differences between neotocite of the groundmass and veinlets were not established. It is noteworthy that at practically similar proportions of cations, the BSE images of groundmass neotocite frequently have a "cloudy" pattern with uneven distribution of areas of irregular shape differing in gray color intensity. Such areas rather differ in the water content and/or density, which is possible in glassy phases.

The composition of the best-studied neotocite that composes the large veinlet in sample Ush318-113 can be considered as the most representative. With allowance for the thermal and chemical data, this neotocite is characterized by the following composition (average of four analyses nos. 4–7 in Table 1, wt %): SiO_2 43.13, Al_2O_3 0.32, MnO^{tot} 41.54, MgO 1.39, CaO 0.90, Na_2O 0.27, H_2O 11.90, total 99.45.

Manganese in the mineral likely occurs mainly (or even completely) in the divalent state. This follows from several independent facts: (1) nearly 100% total of oxide contents (including H_2O) in the presented above chemical composition of mineral; (2) observed change of neotocite color on air, which is likely caused by the oxidation of initially divalent manganese; (3) occurrence of neotocite exclusively in the hausmannite ores in association with minerals that are stable under reducing conditions and low oxygen fugacity: caryopilite, rhodochrosite, tephroite, and hausmannite; under reducing conditions, manganese is usually involved in silicates in the divalent form; (4) replacement of neotocite by rhodochrosite, which is likely possible only under reducing conditions, in the absence of free oxygen. In the oxygen-saturated environment (for instance, in the oxidation zone of ores), rhodochrosite and neotocite are instable and rapidly replaced by Mn^{3+}/Mn^{4+} oxides.

In spite of the glassy structure of neotocite, the silica to manganese ratio in most cases recalculated for atomic amounts is close to Si : Mn ≈ 1 : 1. This affected the ideal neotocite formulas, two versions of which were proposed: $Mn^{2+}(SiO_3)\cdot nH_2O$ (Clark et al., 1978; *Mineraly,* 1992) and $Mn_4^{3+}(Si_4O_{10})(OH)_8\cdot nH_2O$ (Strunz and Nickel, 2001; Krivovichev, 2018, 2021). According to the last formula, neotocite is dominated by trivalent manganese, which, as mentioned above, was hardly probable. The more correct version of the given formula should have the following view: $Mn_4^{2+}(Si_4O_{10})(OH)_4\cdot nH_2O$. However, in any case, the presented above formulas reflect equal atomic amounts of silica and manganese in the neotocite. However, in fact, this is not the case: silicon content in the neotocite is much more than the manganese content. This was mentioned by practically all researchers of neotocite (Clark et al., 1978; Eggleton et al., 1983;

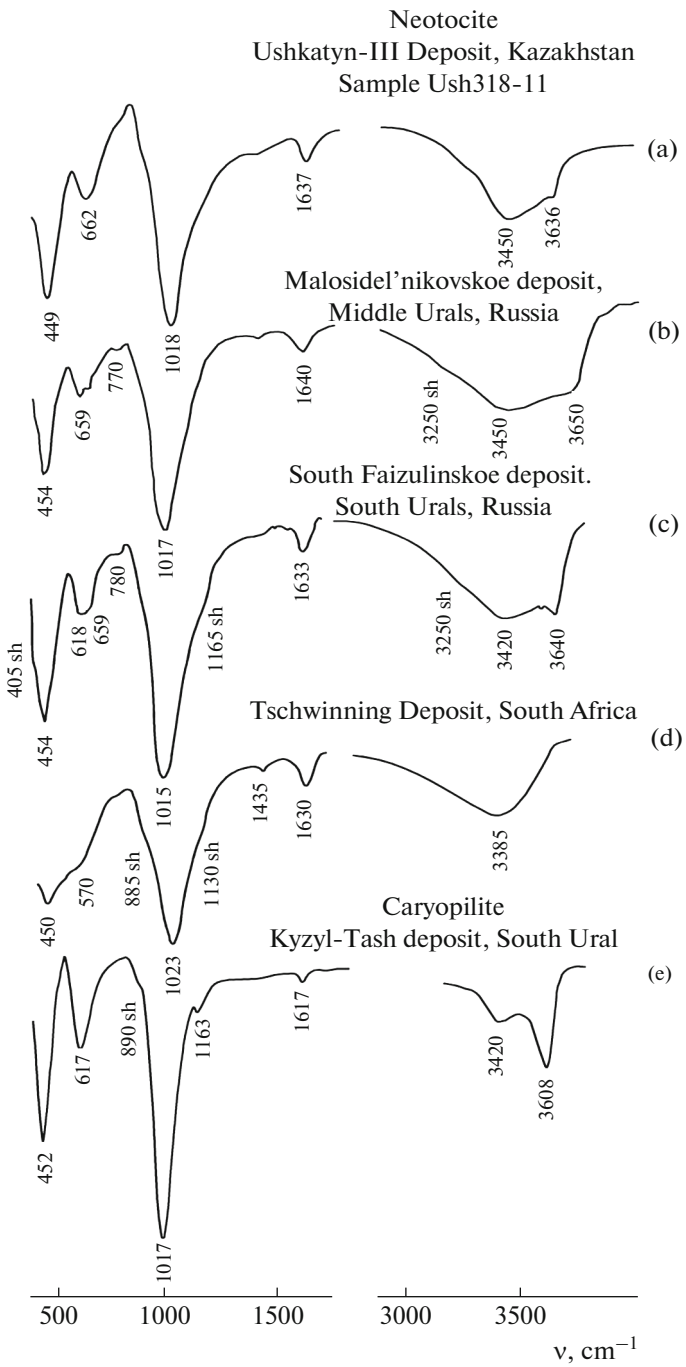

Fig. 5. IR spectra of neotocite (a–d) and caryopilite (e). References: (a–c and e) our data (this work; Brusnitsyn, 2000, 2013; Brusnitsyn et al., 2000), (d) data from (Chukanov, 2014).

Brusnitsyn, 2013), but mineral formulas have not been refined yet.

Obtained data show that (Si + Al) : (Mn + Mg) ratio in the neotocite has nearly normal distribution and varies from 0.95 to 1.40 (Fig. 6). Thereby, the majority of compositions (71%) fall in the much narrower range from 1.10 to 1.25, averaging 1.18. Three last digits are very close to Si : Mn ratios equal 20 : 18, 20 : 16, and 20 : 17, respectively. Converting these values into crystal chemical formulas, with allowance for atomic ratio O : Si = 2.5 typical of layer silicates, the equality of positive and negative charges, as well as the presence of at least two forms of hydrogen-bearing groups in neotockite yield:

Table 1. Chemical composition (wt %) and coefficients of the crystal empirical formulae of neotocite

Components	Sample Ush318-113							Sample Ush318-116						
	Groundmass			Veinlet				Groundmass				Veinlet		
	1	2	3	4	5	6	7	8	9	10	11	12	13	14
SiO_2	42.84	43.22	43.35	43.36	43.49	42.97	42.69	43.52	42.81	42.40	44.4	43.61	43.14	43.51
Al_2O_3	0.00	0.00	0.00	0.33	0.40	0.30	0.24	0.57	0.45	0.32	0.27	0.50	0.44	0.45
MnO*	41.65	41.90	42.69	41.69	41.8	41.18	41.50	43.07	43.04	42.4	43.02	41.45	41.2	41.31
MgO	1.46	1.32	1.35	1.29	1.40	1.39	1.49	1.18	0.82	0.88	0.87	0.97	0.97	1.06
CaO	0.80	0.73	0.82	0.94	0.85	0.94	0.86	0.93	0.8	0.93	1.07	1.12	1.01	1.03
Na_2O	0.00	0.00	0.00	0.30	0.29	0.31	0.18	0.00	0.14	0.14	0.26	0.33	0.27	0.32
Total	86.75	87.17	88.21	87.91	88.23	87.09	86.96	89.27	88.06	87.07	89.89	87.98	87.03	87.68
	Coefficients calculated for 46 charges													
Si	7.95	7.98	7.93	7.93	7.92	7.93	7.91	7.87	7.88	7.89	7.96	7.95	7.96	7.96
Al	0.00	0.00	0.00	0.07	0.09	0.07	0.05	0.12	0.10	0.07	0.06	0.11	0.10	0.10
Total IV**	7.95	7.98	7.93	8.00	8.01	7.99	7.96	7.99	7.97	7.96	8.01	8.06	8.05	8.06
Mn	6.53	6.54	6.60	6.44	6.43	6.42	6.49	6.58	6.69	6.67	6.52	6.39	6.42	6.39
Mg	0.41	0.37	0.37	0.35	0.38	0.38	0.41	0.32	0.23	0.25	0.23	0.27	0.27	0.29
Total VI**	6.94	6.90	6.97	6.80	6.82	6.81	6.91	6.90	6.92	6.91	6.75	6.65	6.69	6.68
Ca	0.16	0.14	0.16	0.18	0.17	0.19	0.17	0.18	0.16	0.19	0.21	0.22	0.20	0.20
Na	0.00	0.00	0.00	0.11	0.10	0.11	0.06	0.00	0.05	0.05	0.09	0.12	0.10	0.11
Total	0.16	0.14	0.16	0.29	0.27	0.30	0.24	0.18	0.21	0.24	0.30	0.34	0.30	0.32

Analyses of neotocite from hausmannite ores varieties, where this mineral is major. * All manganese is taken as divalent; ** total of components supposedly of tetrahedral and octahedral pattern, respectively.

Atomic ratios of Si : Mn	Idealized formula	
	full variant	reduced variant
20 : 18	$Mn_{18}(Si_{20}O_{50})(OH)_{16}\cdot nH_2O$	$Mn_9(Si_{10}O_{25})(OH)_8\cdot nH_2O$
20 : 17	$Mn_{17}(Si_{20}O_{50})(OH)_{14}\cdot nH_2O$	$Mn_{8.5}(Si_{10}O_{25})(OH)_7\cdot nH_2O$
20 : 16	$Mn_{16}(Si_{20}O_{50})(OH)_{12}\cdot nH_2O$	$Mn_8(Si_{10}O_{25})(OH)_6\cdot nH_2O$

Differences in these formulas are insignificant, and their series from the first to third formulas reflects variations of species-forming elements in most part of neotocite analyses. It is reasonable to take $Mn_{17}(Si_{20}O_{50})(OH)_{14}\cdot nH_2O$ as averaged formula. Dividing all coefficients by 2.5 yields $Mn_{6.8}(Si_8O_{20})(OH)_{5.6}\cdot nH_2O$ or, rounding to the nearest integers, $Mn_7(Si_8O_{20})(OH)_6\cdot nH_2O$. This is slightly more simple and convenient version of ideal neotocite formula compared to the above shown. In general, it provides more adequate main features of neotocite constitution, in particular, Si : Mn ratio close to 1 : 1, but with insignificant predominance of silicon (average value of Si : Mn = 1.14), the presence of layer packages in the mineral, and at least two different hydrogen-bearing groups: (OH)-group and H_2O molecules.

Presented above average analysis of neotocite (sample Ush318-113) is well calculated both for the proposed full formula $Mn_{17}(Si_{20}O_{50})(OH)_{14}\cdot nH_2O$ and for the reduced formula $Mn_7(Si_8O_{20})(OH)_6\cdot nH_2O$. In

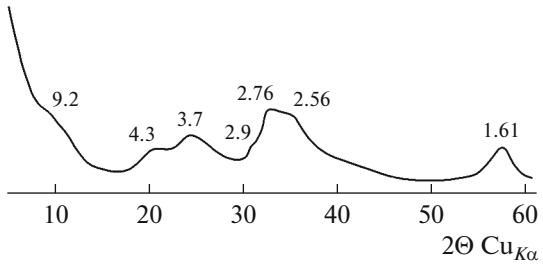

Fig. 6. Powdered X-ray diffraction pattern of a neotocite. Presented data are given for sample Ush318-113. Numerals above peaks are interplanar spacings, in Å.

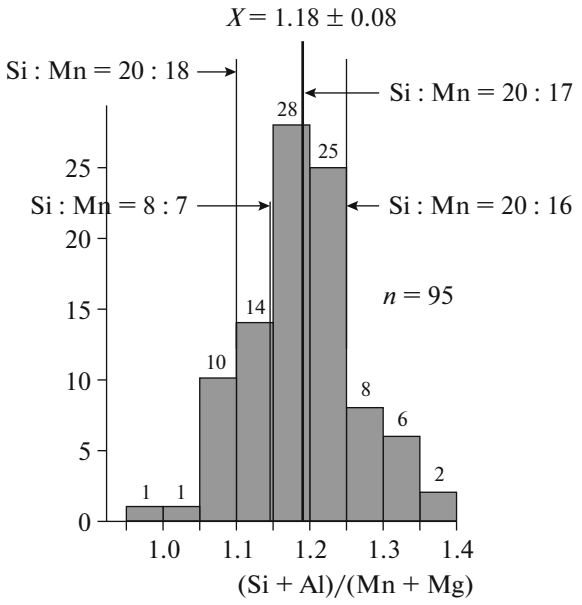

Fig. 7. The ratio of the major element contents in the neotocite composition. *n* (and numerals above columns) is the number of analyses. *X* is mean ± standard deviation.

the latter case, with allowance for the true water content in neotocite, the empirical formula of the mineral has the following view (calculated for 46 charges):

$$(Ca_{0.18}Na_{0.09})_{0.27}(Mn_{6.45}Mn_{0.38})_{6.83} \times [(Si_{7.92}Al_{0.07})_{7.99}O_{20}](OH)_{6.00} \cdot 4.29H_2O.$$

Insignificant deficiency in Mn and Mg (supposedly, octahedrally coordinated cations) is compensated by the incorporation of calcium and sodium in neotocite, as occurs, for instance, in smectites.

Thus, the idealized formula of neotocite can be written as $Mn_7(Si_8O_{20})(OH)_6 \cdot 4H_2O$.

GENETIC INTERPRETATION OF THE RESULTS

The question of neotocite genesis in the studied ores is of great interest and has not yet been definitely resolved. It is obvious that (1) neotocite is formed under low-temperature reducing setting; under oxidizing setting, neotocite is instable and therefore is not observed in association with braunite. (2) Neotocite is formed by devitrification of gel-like manganese–silicate mass. This follows from the glass-like, locally patchy-clumpy structure of neotocite segregations that are split by characteristic syneresis cracks. (3) Judging from the mineral composition and textures of manganese ores, conditions of formation of neotocite (X-ray amorphous phase) clearly differ from those of closely associated minerals (hausmannite, tephroite, caryopilite, rhodochrosite, and others) with perfect crystal structures. For such cases, Chukhrov (1973) used term ephemeral mineral to designate an instable metastable phase observed in thermodynamically atypical conditions. The Ushkatyn neotocite is typical ephemeral mineral. (4) Neotocite is present both in the ore groundmass and in the late veinlets, which should be taken into account in genetic reconstructions. (5) Neotocite is not a mineral of the oxidation zone. It is formed in the ore-bearing sediments under anoxic conditions. Finds of neotocite in oxidized manganese ores sometimes reported in literature (*Mineraly*, 1992) are ambiguous. In these works, a dispersed mixture of oxides of silicon (quartz, opal) and tri- and tetravalent manganese was mistakenly determined as neotocite. It is highly probable that the aggregates of these minerals in some cases are developed after neotocite, inheriting its initially glass-like appearance, which leads to inaccuracies in the mineral identification.

It is most difficult to explain the large neotocite accumulations in the groundmass of the studied ores. Two variants are possible.

Variant 1. Neotocite represents relicts of Mn–Si–H_2O phase (gel?), which has existed in the initial metalliferous sediments and at the diagenetic stage coagulated with formation of manganese–silicate glass. Neotocite of such origin is known in unmetamorphosed sediments. It serves as heavy confirmation for possible accumulation of primary manganese not only in oxide (as usually occurs) but also in silicate form (Aleksiev, 1960; Clark et al., 1978; Andrushchenko et al., 1985; Roi, 1986; *Mineraly,* 1992; Brusnitsyn, 2013). The sedimentary–diagenetic origin is also possible for neotocite from the Ushkatyn-III deposit. The wide development of hydrous manganese silicates in the hausmannite ores, first of all, rock-forming caryopilite and friedelite, definitely indicates the presence of manganese–silicate phase in the initial sediments. The problem is not whether the sediment contained Mn–Si–H_2O phase initially, but whether the neotocite observed in the rocks represents its relict or formed later. It is surprising that sufficiently high amounts of supposedly diagenetic neotocite (manganese–silicate glass) have been preserved in sediments, which were almost completely transformed during the cata- and metagenesis. It is possible that separate areas of ore lodes are situated among rocks that were initially saturated in weakly permeable clay layers. The latter served as screens preventing water removal and thus protecting neotocite from decomposition that is inevitable under the growth of dehydration temperature and pressure and the replacement by minerals with well formed crystal structures.

Variant 2. Neotocite is one of the late hydrothermal minerals forming owing to the rapid "discharge" of pore solutions both in the ore groundmass (filling pores, intergranular space, and partly replacing surrounding minerals) and along the network of cross-cutting fractures. This scenario is possible for low-

neotocite hausmannite ores prevailing at the deposit. However, this mechanism for neotocite-rich ores suggests the intense replacement of previously formed minerals by glassy phase, i.e., significant transformation of rocks with transition of crystalline silicates into amorphous state. At the same time, mineralogical observations show that the neotocite in some ore areas is replaced by caryopilite rather than vice versa. The ores show no clear signs of corrosion of hausmannite, tephroite, pennantite, talc, and rhodochrosite by neotocite. It is however, unknown why neotocite replaces only one silicate, caryopilite. In addition, the sources and mechanisms of influx of great amount of water (required for large-scale formation of neotocite) into narrow localized areas of ore-bearing sediments are not clear yet. The watering of metalliferous sediments could be caused by influx of groundwaters from adjacent areas of sedimentary sequence saturated in clay beds. It is known that the compaction of clay sediments as well as the phase transformations of clay minerals are accompanied by the release of great amount of water. According to estimates by Kholodov (2006), only one montmorillonite to illite transition at the catagenetic stage releases up to 350 km water per 1 m^3 clay. Under favorable combination of water aquifers and reservoir beds, this water could be accumulated in definite horizons and even create zones with excess hydrostatic pressure. It is highly probable that the groundwaters of such genesis drained separate sites of the ore-bearing sequence of the Ushkatyn-III deposit, which led to the low-temperature hydrothermal alteration of manganese deposits already subjected to the cata- and metagenesis. It is also probable that the neotocite was formed owing to the percolation of meteoric groundwaters into deep horizons of ore-bearing deposits. These groundwaters lost dissolved oxygen during manganese oxidation in subsurface parts of the deposit. Thus, the neotocite could be produced by processes in the lowermost zones of weathering crust.

The intermediate "compromise" version is possible, when the efficient development of late hydrothermal neotocite occurs in the rocks that retained relicts of the early diagenetic neotocite and is hardly possible in other ore varieties.

The formation of the neotocite in late veinlets is more clear understood. There, it was segregated from host rock, i.e., represents a peculiar genetic analogue of "alpine-type veins". The development of veinlet network could be related to the tectonic deformations of rocks or was caused by a change of their volume (decompaction) during postsedimentation crystallization of minerals. A rapid filling of open space by manganese- and silicon-saturated pore solutions and precipitation of matter led to the appearance of neotocite. Thereby, the minerals of veins and groundmass in the given case are formed through a single continuous process, while neotocites from ores and late veinlets are genetically related and differ only in morphology.

CONCLUSIONS

Neotocite is a characteristic mineral of low-grade metamorphosed sedimentary manganese ores of the Ushkatyn-III deposit. It occurs both in the ore groundmass, where it associates with hausmannite, tephroite, caryopilite, friedelite, pennantite, rhodochrosite, kutnohorite, and other minerals, and in the cross-cutting veinlets. It is suggested that manganese in neotocite is present mainly (or even completely) in the divalent form. Stoichiometry of the mineral corresponds to the ideal formula $Mn_7(Si_8O_{20})(OH)_6{\cdot}nH_2O$. Neotocite is formed under low temperatures reducing setting. Such conditions occur either during burial of metalliferous sediments containing $Mn–Si–H_2O$ substance (gel?) or later during hydrothermal alteration of the already formed manganese ores.

FUNDING

The studies were performed using analytical facilities of Resource Centers "X-ray Diffraction Methods of Study", "Microscopy and Microanalysis," and "Geomodel" at the St. Petersburg State University.

CONFLICT OF INTEREST

The authors of this work declare that they have no conflicts of interest.

REFERENCES

Aleksiev, B., Neotocite from the Oligocene manganese ore horizon of the Varna region, *Mineral. Sb. L'vov. Geol. O-va.,* 1960, no. 14, pp. 208–214.

Andrushchenko, P.F., Suslov, A.T., and Gavashvili, N.V., Manganese deposits of the Tetritskaro ore region of Georgia, in: *Vulkanogenno-osadochnye i gidrotermal'nye margantsevye mestorozhdeniya (Tsentral'nyi Kazakhstan, Malyi Kavkaz, Eniseiskii kryazh* (Volcanosedimentary and Hydrothermal Manganese Deposits (Central Kazakhstan, the Lesser Caucasus, the Yenisei Ridge), Vitovskaya, I.V., Eds., Moscow: Nauka, 1985, pp. 115–172.

Brusnitsyn, A.I., *Rodonitovye mestorozhdeniya Srednego Urala (mineralogiya i genezis)* (Rhodonite Deposits of the Middle Urals: Mineralogy and Genesis), St. Petersburg: Izvo S.-Peterb. Univ., 2000.

Brusnitsyn, A.I., *Mineralogiya margantsevonosnykh metaosadkov Yuzhnogo Urala* (Mineralogy of Manganese-Bearing Metasediments of the South Urals), St. Petersburg: SPbGU, IPK KOSTA", 2013.

Brusnitsyn, A.I. and Chukanov, N.V., Conditions of formation and character of metamorphic transformation of neotocite, *Nekristallicheskoe sostoyanie tverdogo mineral'nogo veshchestva* (Non-Crystalline State of Solid Mineral Matter), Yushkin, N.P., Ed., Syktyvkar: In-t geologii Komi Nauch. Ts. Ural. Otd. RAN; Geoprint, 2001, pp. 106–110.

Brusnitsyn, A.I., Belogub, E.V., Platonova, N.V., Shilovskikh, V.V., and Zhukov, I.G., Aluminum–magnesium variety of caryopilite from goethite–neotocite–rhodochro-

site ores of the Mazulskoe manganese deposit (Krasnoyarsk region), *Zap. Ross. Mineral. O-va,* 2018, no. 6, pp. 90–103.

Brusnitsyn, A.I., Kuleshov, V.N., Sadykov, S.A., Perova, E.N., and Vereshchagin, O.S., Isotopic composition ($\delta^{13}C$ and $\delta^{18}O$) and genesis of Mn-bearing sediments in the Ushkatyn-III deposit, Central Kazakhstan, *Lithol. Miner. Resour.,* 2020, vol. 55. N 6. P. 445–467.

Brusnitsyn, A.I., Perova, E.N., Vereshchagin, O.S., Britvin, S.N., Platonova, N.V., and Shilovskikh, V.V., The Mineralogy of Iron and Manganese Ores of the Ushkatyn-III Deposit in Central Kazakhstan, *Geoil. Ore Deposits,* 2021a, no. 1, pp. 1–29.

Brusnitsyn, A.I., Perova, E.N., Vereshchagin, O.S., and Vetrova, M.N., Geochemical features and accumulation conditions of Mn-bearing sediments in the complex (Fe–Mn and $BaSO_4$–Pb) Ushkatyn-III Deposit, Central Kazakhstan, *Geochem. Int.,* 2021b, vol. 59, no. 9, pp. 858–888.

Buzmakov, E.I., Shibrik, V.I., Rozhnov, A.A., Sereda, V.Ya., and Radchenko, N.M., Stratiform ferromanganese and base metal deposits of the Ushkatyn ore field (Central Kazakhstan), *Geol. Rudn. Mestorozhd.,* 1975, no. 1, pp. 32–46.

Chukanov, N.V., *Infrared Spectra of Mineral Species,* Dordrecht: Springer, 2014.

Chukhrov, F.V., Ephemeral minerals, *Priroda,* 1973, no. 9, pp. 126–133.

Chukhrov, F.V., Gorshkov, A.I., and Drits, V.A., *Gipergennye okisly margantsa* (Supergene Manganese Oxides), Moscow: Nauka, 1989.

Clark, A.M., Easton, A.J., and Jones, G.C., A study of the neotocite group, *Mineral. Mag.,* 1978, vol. 42, pp. M26–M30.

Eggleton, R.A., Pennington, J.H., Freeman, R.S., and Threadgold, I.M., Structural aspect of the hisingerite–neotocite series, *Clay. Mineral.,* 1983, vol. 18, no. 1, p. 21.

Kalinin, V.V., Complex ferromanganese and zinc-lead-barite ores in the Ushkatyn group deposits (central Kazakhstan), In: *Vulkanogenno-osadochnye i gidrotermal'nye margantsevye mestorozhdeniya* (Volcanosedimentary and Hydrothermal Manganese Deposits), Vitovskaya, I.V., Ed., Moscow: Nauka, 1985, pp. 5–6.

Kayupova M.M. *Mineralogiya zheleznykh i margantsevykh rud Zapadnogo Atasu (Tsentral'nyi Kazakhstan)* (Mineralogy of Iron and Manganese Ores in Western Atasu: Central Kazakhstan), Alma-Ata: Nauka, 1974.

Kholodov, V.N., *Geokhimiya osadochnogo protsessa* (Geochemistry of the Sedimentary Process), Moscow: GEOS, 2006.

Krivovichev, V.G., *Mineralogicheskii slovar* (Mineralogical Glossary), St.Petersburg: St. Petersburg Univ., 2009.

Krivovichev, V.G., *Mineral'nye vidy* (Mineral Species), St. Petersburg: St.Petersburg Univ., 2021.

Mineraly: spravochnik (Minerals: a Textbook), Smolyaninova, N.N., Ed., Moscow: Nauka, 1992, vol. 4, no. 2.

Nordenskiöld, N., *Üeber das Atomistisch-Chemische Mineral System und das Examinations-System der Mineralien,* Helsingfors, 1849.

Povondra, P., Minerals of the hisingerite–neotocite series from Chvaletice Zelezne hory Mts., eastern Bohemia, Czech Republic, *J. Czech Geol. Soc.,* 1992, vol. 41/1–2, pp. 7–14.

Roy, S., *Manganese Deposits,* London: Academic Press, 1981.

Rozhnov, A.A., Comparative characteristics of manganese deposits of the Atasuysky and Nikopol-chiatursky types, in *Geologiya i geokhimiya margantsa* (Geology and Geochemistry of Manganese), Varentsov, I.M., Ed., Moscow: Nauka, 1982, pp. 116–121.

Strunz, H. and Nickel, E.H., *Strunz Mineralogical Tables,* Stuttgart: Schweizerbartsche Verlagsbuchhandlung, 2001.

Wheland, J.A. and Goldich, S.S., New data for hisingerite and neotocite, *Am. Mineral.,* 1961, vol. 46, pp. 1412–1423.

Translated by M. Bogina